Low refractive index Si nanopillars on Si substrate

Gong-Ru Lin, Ya-Chung Chang, En-Shao Liu, Hao-Chung Kuo, and Huang-Shen Lin

---

Articles you may be interested in

Omnidirectional reflectance and vanishing Brewster angle of disordered semiconductor nanopillar surface with gradually changed refractive index
J. Appl. Phys. **109**, 083523 (2011); 10.1063/1.3561491

Optical transmission of periodic annular apertures in metal film on high-refractive index substrate: The role of the nanopillar shape
Appl. Phys. Lett. **96**, 201101 (2010); 10.1063/1.3427390

Optical index profile of nonuniform depth-distributed silicon nanocrystals within SiO 2
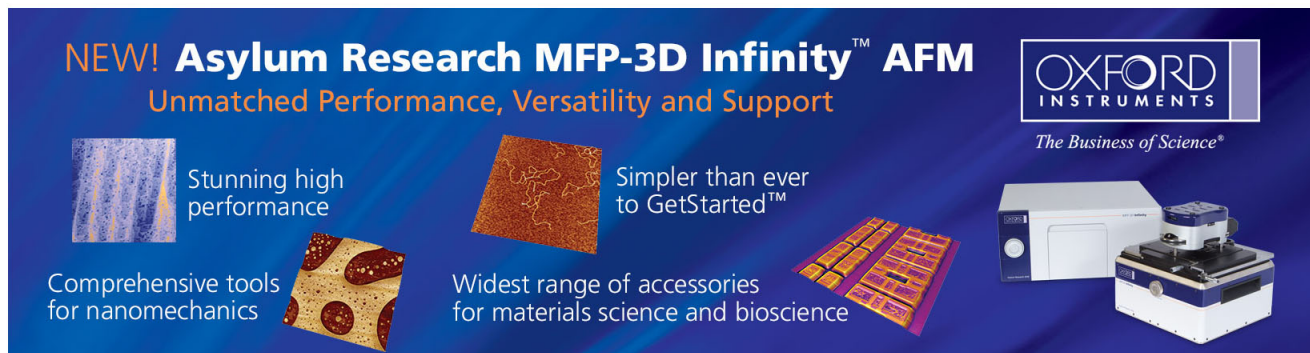J. Appl. Phys. **105**, 013521 (2009); 10.1063/1.3041155

Temperature dependent refractive index of amorphous silicon determined by time-resolved reflectivity during low fluence excimer laser heating
J. Appl. Phys. **99**, 063516 (2006); 10.1063/1.2186378

Size dependence of refractive index of Si nanoclusters embedded in SiO 2
J. Appl. Phys. **98**, 013523 (2005); 10.1063/1.1943512

Low refractive index Si nanopillars on Si substrate

Gong-Ru Lin[a)]
Graduate Institute of Electro-Optical and Department of Electrical Engineering, National Taiwan University, No. 1, Roosevelt Road Sec. 4, Taipei 106, Taiwan, Republic of China

Ya-Chung Chang and En-Shao Liu
Research Center for Applied Sciences, Academia Sinica, 128 Academia Rd., Sec. 2 Nankang, Taipei 115, Taiwan, Republic of China

Hao-Chung Kuo and Huang-Shen Lin
Department of Photonics, National Chiao Tung University, 1001, Ta Hsueh Road, Hsinchu 300, Taiwan Republic of China

Low refractive index of a stalagmitelike high-aspect-ratio Si nanopillar array on Si dry etched using a self-aggregated Ni nanodot mask is demonstrated, which exhibits two minimum reflectances of 1.23 and 1.4 with corresponding refractive indices of 1.25 and 1.48 at 400 and 1200 nm, respectively. Angular dependency of the transverse electrical mode reflectance at 632.8 nm of the surface roughened Si nanopillar array is released, and the Brewster angle of 63° with equivalent refractive index of 1.5 is determined. © *2007 American Institute of Physics.*
[DOI: 10.1063/1.2736281]

Versatile nanoscale silicon (Si) or silica structures with extraordinary electrical and optical characteristics have recently been synthesized and investigated, such as porous Si[1] or nanoporous silica,[2] Si nanopyramid,[3] Si nanopillar,[4,5] or silica nanorod[6,7] array on Si substrate. These surface roughened nanostructures are considered as promising systems for developing electronic or photonic devices. Enhanced optical phonon response, variable selection rules, and a low-frequency shift of 0.5 cm^{-1} of Raman band corresponding to the quantum size effect in Si nanorods were observed.[8] In particular, the modified optical refractive index of the aforementioned Si or silica nanostructures is of great interest, which plays an important role on the performance of Si based photonic devices involving high-reflection or antireflection multilayer coating, resonant cavity, and photonic crystal structures.[6,7] Another demand for potential application in Si based photovoltaic solar cells also becomes a driving force for emerging Si or silica nanostructures of ultralow refractive indices. Not long ago, the silica nanorod array on Si substrate with unprecedented refractive index of 1.08,[7] even smaller than those of the MgF_2, CaF_2, and SiO_2 films used for depositing antireflection coatings, were demonstrated in visible spectral range. Nonetheless, the study on reflectance or refractive index spectroscopy of a similar Si nanopillar structure was seldom addressed. In this work, we investigate the optical reflectance spectroscopy of a Si nanopillar array fabricated using a Ni nanodot mask assistant reactive-ion-etching process. Ultralow refractive index in the UV-visible-near infrared wavelength range in comparison with other dielectric materials is demonstrated and elucidated.

A Ni/SiO_2 nanomask assistant dry-etching procedure is employed to fabricate the Si nanopillars on Si substrate, as schematically shown in Fig. 1. A 50-nm-thick Ni film is evaporated on the SiO_2/Si substrate using an e-beam evapo-

rating system with Ni deposition rate of 0.1 Å/s under an applied current of 70 mA. The SiO_2 buffered layer with a thickness of 200 Å is deposited by using a plasma enhanced chemical vapor deposition under standard recipe. Subsequently, a rapid thermal annealing process at 850 °C for 22 s under the N_2 flowing gas of 5 SCCM (SCCM denoted cubic centimeter per minute of STP) is performed to self-aggregate the Ni nanodots on SiO_2/Si substrate. By using the Ni nanodots with area density of 5×10^{11} cm^{-2} as a nanomask, the Si substrate is dry etched in a planar-type inductively coupled plasma–reactive ion etching (ICP-RIE) system (SAMCO ICP-RIE 101iPH) at rf frequency of 13.56 MHz and the ICP/bias power conditions of 100/50 Watts. The etching gases of CF_4 and Ar mixture with a condition of $CF_4/Ar = 40/40$ SCCM were introduced into the reactive chamber through individual electronic mass flow controllers. The chamber pressure of 0.66 Pa remains unchanged during an etching duration of 5–7 min. To avoid the gradual oxidation effect, the Si sample is dipped in methyl alcohol before diagnosis. The sample is dried with a 2 min nitrogen purge prior to the measurement. The surface reflectance of the Si nanopillars on Si substrate is characterized at wavelength
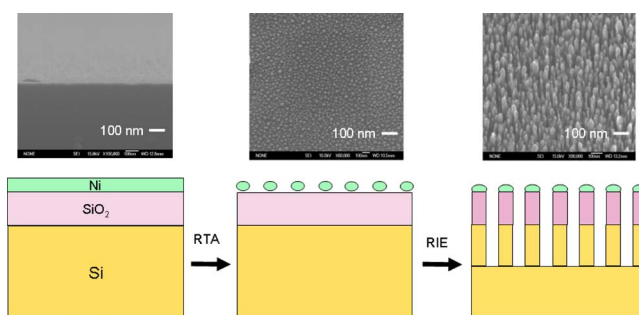

FIG. 1. (Color online) Schematic diagram for fabricating Si nanopillar array on Si using a self-assembled Ni nanodot etching mask on SiO_2/Si substrate is illustrated. The scanning electron microscopic (SEM) photographs of unprocessed Si substrate, self-aggregated Ni on SiO_2/Si, and ICP-RIE etched Si nanopillars on Si are shown for example.

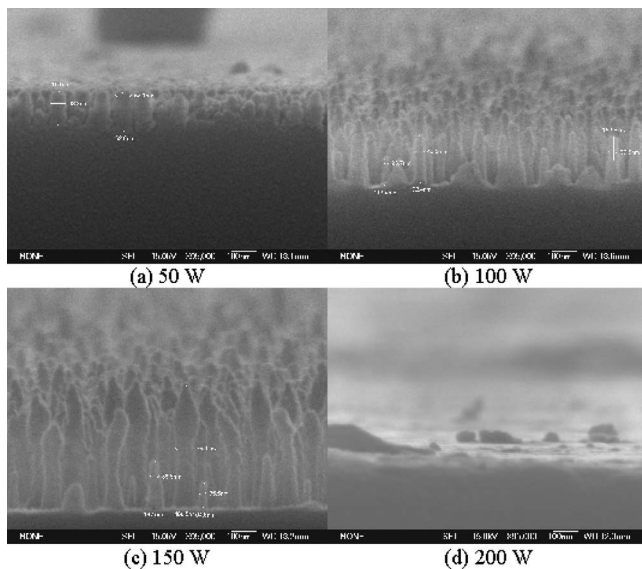a)Author to whom correspondence should be addressed; electronic mail: grlin@ntu.edu.tw

FIG. 2. SEM photographs of Si nanopillar array obtained by detuning the ICP power at (a) 50, (b) 100, (c) 150, and (d) 200 W.
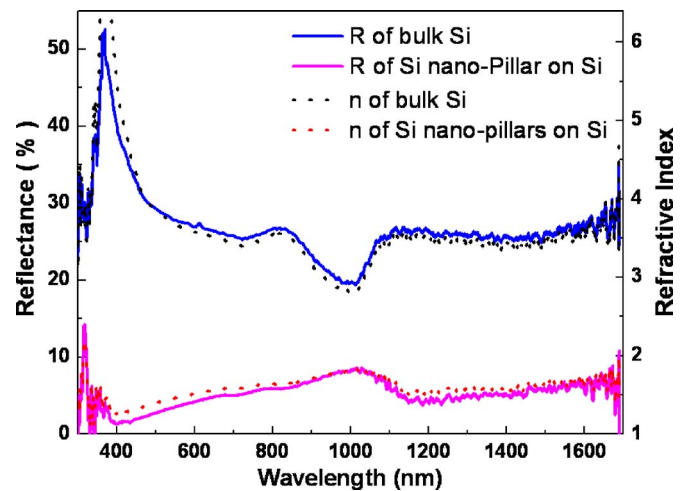

FIG. 3. (Color online) Surface reflectance and corresponding refractive indices of unprocessed bulk Si and Si nanopillar array on Si substrate.

ranging from 300 to 1700 nm. After removing the Ni/SiO$_2$ nanomask, the Si nanopillars with a perpendicular sidewall and high aspect ratio are obtained, as shown in Fig. 1. The density, diameter, and height of Si nanopillars are tunable from 6.5×10^{10} to 5×10^{11} cm^{-2}, from 30 to 70 nm, and from 100 to 480 nm, respectively. Figure 2 clearly shows that the ICP power of the ICP-RIE strongly affects the etching rate and substrate selectivity. At an ICP power of 50 W, the etching selectivity is high but the etching rate is very low, leading to the incompletely formatted Si nanopillars with average height of 100 nm and extremely low aspect ratio of <2 shown in Fig. 2(a). Increasing ICP power to 100 W results in a compromise between substrate selectivity and etching rate, providing a higher Si nanopillar (>180 nm) with smaller size (<35 nm) and enhanced aspect ratio of 5. Such a trade-off between the etching rate and the aspect ratio becomes less significant at ICP power ranging between 100 and 150 W. The etching depth reaches its maximum at ICP power of 150 W, providing a Si pillar array as high as 480 nm with its aspect ratio ranging from 5 to 8, as shown in Fig. 2(c). Afterwards, Fig. 2(d) illustrates that the Si nanopillars were etched out due to the low etching selectivity and high etching rate at ICP power higher than 200 W.

The Si nanopillar array with highest aspect ratio was selected to characterize its optical reflectance spectroscopy and to compare with that of bulk Si substrate, as shown in Fig. 3. As a result, the reflectance of Si wafer decreases after nanomask formation and nanopillar etching. It is observed that the Si nanopillar array on Si substrate has a maximum reflectance $<8.6\%$ (at 1013 nm), corresponding to a refractive index of <1.82 at wavelength ranging from 320 to 1650 nm. However, it is already much smaller, less than that of the unprocessed Si substrate (see Fig. 3). In comparison, the standard silica coating exhibits a reflectance of 5.2% and a refractive index around 1.4 within the wavelength region. In the visible spectral range, MgF$_2$, CaF$_2$, and SiO$_2$ with refractive indices of 1.39, 1.44, and 1.46, respectively, are currently available candidates with lowest refractive indices.[6,7] In particular, the Si nanopillar array has ultralow refractive indices of 1.23 and 1.4 at two wavelength regions around 400 and 1200 nm, respectively. The Si nanopillar array roughened surface inevitably causes a reflectance lower than that of the Si substrate on account of its highly roughened surface.[7] We also experimentally found that the Si nanopillars encapsulated with Ni and SiO$_2$ nanomask exhibit even lower reflectance than the pure Si nanopillar array due to the existence of oxide nanodots. In contrast to the traditional antireflection coatings for Si-based photon energy transforming devices using optically homogeneous materials with a refractive index lower than that of a cell semiconductor, such a low-reflectance Si nanopillar array further motivates the development of Si nanomaterials which benefits from fully processing compatibility with the Si based photovoltaic solar cell. On the other hand, the emergence of the nanostructural materials also provides flexibility on gradually detuning the refractive index between 1.2 in vacuum and 3.9 in bulk Si at visible wavelengths. Recently, an optical film consisting of SiO$_2$ nanorod array have been demonstrated to show ultralow refractive index of 1.08 with a film thickness of 1.35 μm,[7] in which the angled SiO$_2$ nanorods with both the gap spacing and diameter are much smaller than the wavelength of visible light to minimize Mie and Rayleigh scattering. Moreover, similar antireflection phenomenon was also found on the porous Si surface, revealing a reduced refractive index of 1.75–2.15.[1] In our case, a refractive index of 1.23 at 400 nm is obtained in the Si nanopillar array on Si substrate with an average height of only 450 nm.

To realize the antireflection property of the Si nanopillar array on the bulk Si substrate for potential application on photovoltaic solar cells, we further characterize the angular dependent reflectance by using TE and TM polarized beams of a HeNe laser at 632.8 nm. The angular dependent reflectance at different incident polarizations in Fig. 4 shows similar low-reflectance phenomenon with that of the silica nanopillar array observed by Xi *et al.*[7] previously. The Brewster angle of the bulk Si related to a minimum reflectance of 8.21×10^{-2} for the TE-mode laser beam is determined as 76°. Possible mechanism of the slightly deviated Brewster angle as well as refractive index measured from the unprocessed Si wafer is mainly attributed to the contribution of the surface oxide layer naturally grown on the unprocessed Si substrate. In contrast, the Si nanopillar array exhibits ex-
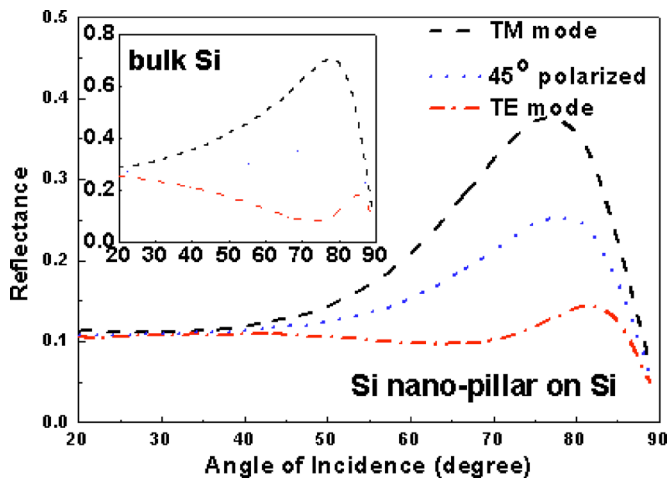
FIG. 4. (Color online) Angular dependent reflectance of Si nanopillar array and bulk Si substrate (inset) measured by HeNe laser at 632.8 nm and different polarizations.

tremely low TE-mode reflectance of $<1 \times 10^{-1}$ associated with a change in reflectance of only 0.016 at incident angles $<75°$. With the formula of $\theta_{\text{Brewster}} = \tan^{-1}(n_{\text{si}}/n_{\text{air}})$, the determined Brewster angle with a minimum reflectance of 9.05×10^{-2} is about 63°, corresponding to an equivalent refractive index of only 1.5 at wavelength of 632.8 nm for such a high-aspect-ratio Si nanopillars on Si substrate. The calculated refractive index is relatively in good agreement with that obtained from the reflectance spectroscopy (see Fig. 3). Another direct evidence to support the ultralow refractive index of the Si nanopillar array is its greatly reduced reflectance at lower incident angles as compared to the unprocessed bulk Si substrate. For example, the reflectance of Si substrate at an incident angle of 20° is significantly reduced from 29.5% to 10.5% after formatting Si nanopillars, corresponding to a refractive index changing from 3.378 to 1.958. Identical trend can also be obtained under both the 45°-polarized and TE-mode incident conditions. The more important observation is that the Si nanopillar array exhibits a less angle-dependent TE-mode reflectance in comparison with the bulk Si substrate, which indicates that the polarization dependence of reflectance has been released by introduc-

ing such a surface roughened Si nanopillar array on Si substrate.

In conclusion, we have investigated the reflectance spectroscopy of Si nanopillar array on Si substrate with high aspect ratio. The stalagmitelike Si nanopillar array is fabricated by dry etching the SiO_2/Si substrate with self-aggregated Ni nanodot array based etching mask. The density, diameter, and height of Si nanopillars are tunable from 6.5×10^{10} to 5×10^{11} cm^{-2}, from 30 to 70 nm, and from 100 to 480 nm, respectively. The Si nanopillar array inevitably causes a reflectance lower than that of the Si substrate on account of its air/Si mixed structure and highly roughened surface, leading to an ultralow reflectance of $<8.6\%$ (at 1013 nm) and corresponding refractive index of <1.82 at wavelength ranging from 320 to 1650 nm. A minimum reflectance and refractive index of 1.23 and 1.25 at wavelength of 400 nm is obtained for the Si nanopillar array on Si with average height of 450 nm and aspect ratio of 5. The Brewster angle of 63° obtained by TE-mode angular dependent reflectance at 632.8 nm gives rise to an equivalent refractive index of nearly 1.5, which is relatively in good agreement with the reflectance spectroscopic analysis. The angular reflectance further reveals a released polarization dependency of such a surface roughened Si nanopillar array on Si substrate.

[1] E. Chambon, E. Florentin, T. Torchynska, J. Gonzalez-Hernandez, and Y. Vorobiev, Microelectron. J. **36**, 514 (2005).
[2] G. Wu, J. Wang, J. Shen, T. Yang, Q. Zhang, B. Zhou, Z. Deng, B. Fan, D. Zhou, and F. Zhang, Mater. Sci. Eng., B **78**, 135 (2000).
[3] G.-R. Lin, H.-C. Kuo, H.-S. Lin, and C.-C. Kao, Appl. Phys. Lett. **89**, 073108 (2006).
[4] T. Tada, A. Hamoudi, T. Kanayama, and K. Koga, Appl. Phys. Lett. **70**, 2538 (1997).
[5] T. Tada and T. Kanayama, J. Vac. Sci. Technol. B **16**, 3934 (1998).
[6] S.-Y. Lin, E. Chow, V. Hietala, P. R. Villeneuve, and J. D. Joannopoulos, Science **282**, 274 (1998).
[7] J.-Q. Xi, J. K. Kim, and E. F. Schubert, Nano Lett. **5**, 1385 (2005).
[8] V. V. Poborchii, T. Tada, and T. Kanayama, Physica E (Amsterdam) **7**, 545 (2000).